Vibrational Microspectroscopy and Imaging of Molecular Composition and Structure During Human Corneocyte Maturation

Guojin Zhang[1], David J. Moore[2], Richard Mendelsohn[1] and Carol R. Flach[1]

The outermost region of the epidermis, the stratum corneum (SC), provides an essential barrier to water loss and protects against exogenous substances. The functional integrity of the SC depends on a complex maturation and exfoliation process, which is often perturbed in skin diseases. The maturation of corneocytes isolated from different depths in healthy human SC was investigated using infrared (IR) spectroscopic imaging and Raman microscopy. Both IR and Raman spectral quality of individual corneocytes was high and revealed depth-dependent variations in molecular composition. Spectral changes were identified as arising from alterations in the concentration of the major constituents of natural moisturizing factor (NMF), important in maintaining SC hydration. A significant decrease in the concentration of NMF was observed for corneocytes isolated from superficial compared to deeper SC layers (layer 3 vs. layer 11, respectively). An IR parameter that measures the relative NMF concentration in corneocytes is introduced. The potential role of vibrational imaging to evaluate corneocyte composition and molecular structure in the treatment of NMF-related diseases is discussed.

Journal of Investigative Dermatology (2006) **126,** 1088–1094. doi:10.1038/sj.jid.5700225; published online 2 March 2006

INTRODUCTION

The superficial region of the epidermis, the stratum corneum (SC), provides a vital physical barrier that protects against external insult and maintains water homeostasis. Indeed, a primary function of the epidermis is to generate the SC. The basic structure of this thin ($\sim$10–20 μm) outer layer consists of keratin-rich corneocytes embedded in a highly ordered lipid lamellar phase, analogous in macroscopic architecture to a brick wall (Elias, 1991; Schaefer and Redelmeier, 1996). The hydration level in the SC, although low compared to the underlying viable epidermis and dermis, is key to proper skin barrier function. Water activity is thought to influence the maturation of the SC via its impact on enzyme activity and lipid phase behavior. Continual renewal of the SC is also essential for its functional integrity.

Corneocytes are generated from terminally differentiated keratinocytes as the cells make their way from the stratum granulosum into the SC. During this transition, profilaggrin, a large, insoluble protein, is converted to filaggrin, which is associated with the corneocyte keratin filaments in the deepest layers of the SC. Further processing of filaggrin appears to be driven by the water gradient within the SC and in healthy skin, the relatively low hydration level promotes proteolysis of the protein into its constituent amino acids, amino-acid derivatives, and salts (Scott and Harding, 1986). The resulting mixture, known as natural moisturizing factor or NMF, is highly water soluble and can be as much as 10% of corneocyte dry weight. Atmospheric water is absorbed by the hygroscopic NMF providing sufficient hydration to help keep skin flexible and to facilitate various enzymatic reactions in the pathway that terminates with corneocyte desquamation (Rawlings *et al.*, 1994). The molecular nature of this complex process in healthy and diseased skin continues to be a focus of skin research.

The aforementioned processes have been investigated with cell culture and immunohistochemical techniques. In addition, various optical microscopic methods have been developed to characterize the morphology of the SC and underlying epidermis in healthy and diseased skin. Techniques such as confocal laser scanning microscopy (Langley *et al.*, 2001; Gerger *et al.*, 2005) and two-photon fluorescence microscopy (So *et al.*, 2000; Hanson *et al.*, 2002; Yu *et al.*, 2003) can be applied in a noninvasive manner, avoiding the need to microtome thin sections while achieving high spatial resolution (to the submicron level). Optical microscopic techniques have the potential to become routine diagnostic tools, although molecular level information is limited and exogenous probes may perturb native skin.

[1]*Department of Chemistry, Newark College of Arts and Sciences, Rutgers University, Newark, New Jersey, USA and* [2]*International Specialty Products, Wayne, New Jersey, USA*

Correspondence: Dr Carol R. Flach, Department of Chemistry, Newark College of Arts and Sciences, Rutgers University, 73 Warren Street, Newark, New Jersey 07102, USA. E-mail: flach@andromeda.rutgers.edu

Abbreviations: IR, infrared; NMF, natural moisturizing factor; SC, stratum corneum

Received 20 September 2005; revised 21 December 2005; accepted 10 January 2006; published online 2 March 2006

Vibrational spectroscopic imaging and microscopy offer significant advantages in this regard. Probe molecules are unnecessary and the techniques are sensitive to molecular composition, structure, and interactions among molecular components. However, spatial resolution is lower than in fluorescence-based methods (i.e., ~10 μm in the infrared (IR) and 1–3 μm in the Raman) and the depth of sampling is limited as well. Confocal Raman microscopic measurements can be performed on intact skin to depths of ~100–150 μm (Caspers *et al.*, 2003; Xiao *et al.*, 2004, 2005). In general, microtomed samples (~5 μm thick) are required for IR imaging.

Recent advances in IR spectroscopic imaging and confocal Raman microspectroscopy have permitted the acquisition of spatially resolved chemical composition and structural information from biologically important samples (for reviews, see Salzer *et al.* (2000) and *Vibr Spectrosc* 2005; 38) The variety of biological samples and methods have expanded from tissues and fixed cells to living cells (Moss *et al.*, 2005). Challenges in data collection and interpretation are being confronted and surmounted as the work moves from serving as an adjunct to histopathology to playing a more predictive role in diagnosing disease, providing insights into the molecular interactions preceding the onset of disease, and tracking the effectiveness of therapeutics on a molecular level.

In the current study, the maturation process of individual human corneocytes obtained from different depths in the SC was investigated using IR spectroscopic imaging and Raman microspectroscopy. The results from experiments conducted on cells isolated from healthy skin reveal depth-dependent compositional differences and provide an initial baseline from which an examination of the variability among subjects, body sites, age, and a variety of disease states can be made.

RESULTS

A visual micrograph of several unstained corneocytes isolated from the 11th tape strip is presented in Figure 1a. The corneocytes display characteristic polygonal shapes and sizes. An image of the IR Amide I band (~1650 cm^{-1}) intensity for a single corneocyte from the same layer is shown in Figure 1b, the outer edges of which also display typical corneocyte size. In the image, brightness corresponds to a more intense Amide I band. The small square (solid line) within the IR image denotes the pixel (6.25 × 6.25 μm) from which the spectrum shown to the right (labeled 11th) was acquired. A representative IR spectrum from the 3rd tape strip is also presented in Figure 1c. The spectral features provide information about the composition of the cells and the molecular structure of particular constituents. The spectra demonstrate high signal-to-noise ratios. Only a linear baseline correction was applied to the spectra before statistical and additional analysis. Several strong bands characteristic of proteins and lipids are observed in the spectra including, N–H stretching or Amide A (~3280 cm^{-1}), CH_2 and CH_3 stretching (2840–3000 cm^{-1}), Amide I (predominantly peptide bond C=O stretch at ~1650 cm^{-1}), and Amide II (~60% N–H bend and 40% C–N stretch at ~1550 cm^{-1})

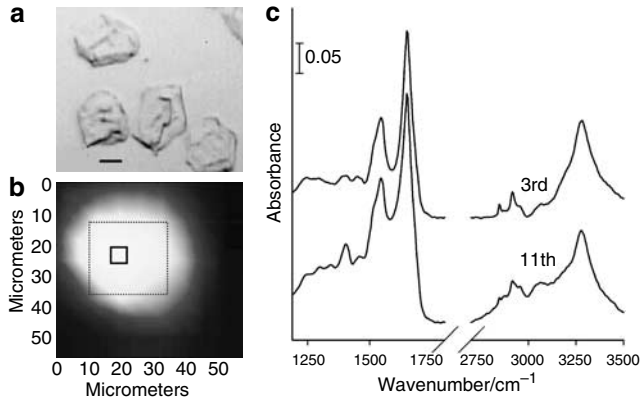

Figure 1. Optical and IR imaging of human corneocytes. (**a**) Optical image of several unstained corneocytes isolated from the 11th tape strip. Bar = 20 μm. (**b**) IR image of Amide I band intensity at 1650 cm^{-1} for a single corneocyte from an 11th layer tape strip. The brighter areas in the image correspond to higher Amide I band intensities. The large box (dashed line) drawn in the center of the image marks the 4 × 4 pixel area (25 × 25 μm) from which corneocyte spectra were analyzed. The small box (solid line) marks the single pixel from which the corresponding spectrum shown in (**c**) was obtained. (**c**) Representative IR spectra (1180–1750 cm^{-1} and 2750–3500 cm^{-1} region) of corneocytes isolated from the 11th (bottom spectrum) and 3rd (top spectrum) tape strips. Each spectrum was obtained from a single 6.25 × 6.25 μm pixel.

bands. In addition, a fairly strong band is observed at ~1400 cm^{-1} only in the spectrum of the corneocyte obtained from the 11th tape strip. The origin of this band and other differences between corneocytes isolated from two depths within the SC will now be more closely examined.

IR images were acquired from multiple corneocytes isolated from the 3rd and 11th tape strips. The images were spatially masked by selecting a 4 × 4 pixel area from the center of each corneocyte as depicted by the dashed box drawn in Figure 1b. In this way, intensity variations owing to edge effects are minimized. A mean spectrum was calculated from the masked images acquired of 36 corneocytes isolated from each layer. Mean spectra (1180–1430 cm^{-1}) along with a difference spectrum (layer 11 − layer 3) are shown in the top of Figure 2a. Before subtraction, the mean spectra were normalized with respect to the intensity of the band observed at ~1245 cm^{-1}. This procedure also effectively normalized the spectra with respect to both the Amide I and II modes (shown before normalization in Figure 2b). Thus, the band at 1245 cm^{-1} is reasonably assigned to the peptide bond Amide III mode (Krimm and Bandekar, 1986). In Figure 2a, significant differences are observed between the two mean spectra, the most prominent being the increased intensity in the band at 1404 cm^{-1} in the spectrum acquired from corneocytes isolated from the deeper layer. The carboxylate symmetric stretching mode absorbs in this spectral region. As the breakdown products of filaggrin (NMF), for example, amino-acid salts and ionized carboxylic acid derivatives, are rich in this functional group, a spectrum was acquired of a dried film consisting of major NMF components (Figure 2a, bottom spectrum). The features observed in the difference

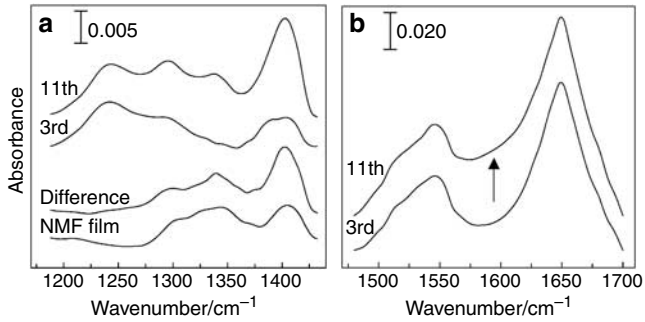

Figure 2. Mean IR imaging spectra of multiple corneocytes from two depths in human SC compared to IR spectrum of model NMF film. (**a**) Mean IR spectra (1180–1430 cm^{-1} region) of 36 corneocytes isolated from 11th layer and 3rd layer tape strips (top two spectra) along with the difference spectrum (11th−3rd) and a spectrum of a model NMF film. (**b**) Mean IR spectra from the same two layers in the Amide I and II region. The arrow marks the approximate position of the asymmetric carboxylate stretching mode.

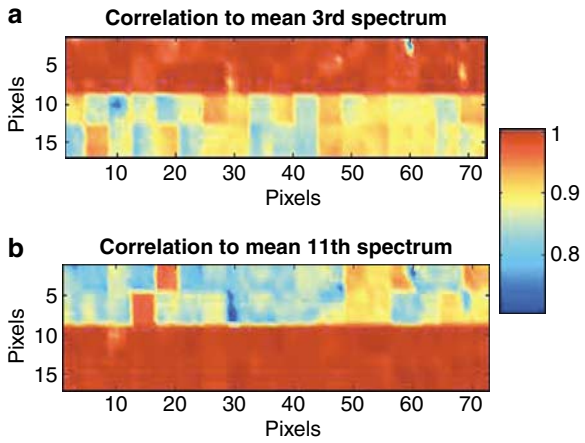

Figure 3. Correlation coefficient images of multiple corneocytes from two depths in human SC. Spatially masked (4 × 4 pixel area) concatenated IR images of correlation coefficients calculated for 72 corneocytes. In each image, the top two rows (total of 8 pixels vertically) contain correlation coefficients for corneocytes isolated from 3rd layer tape strips and the bottom two rows are for corneocytes from 11th layer tape strips. (**a**) Correlation to the mean spectrum (1180–1430 cm^{-1} region) from the 3rd layer. (**b**) Correlation to the mean spectrum (1180–1430 cm^{-1} region) from the 11th layer. The color bar shows the range of calculated correlation coefficients.

spectrum are quite comparable to those in the spectrum of the dried film, thus corroborating assignment of the band at 1404 cm^{-1} to the carboxylate symmetric stretch of NMF constituents. Qualitatively, the concentration of NMF in corneocytes appears to increase significantly with SC depth for the outermost ~11 layers.

Mean corneocyte spectra displayed over the 1480–1700 cm^{-1} region in Figure 2b also support NMF depth-dependent concentration differences as evidenced by increased intensity in the corresponding carboxylate asymmetric stretching region (~1590 cm^{-1}) observed for corneocytes from the deeper SC layer. This appears to be the major difference between the spectra shown in Figure 2b where the Amide I and II band shape and position are very similar for the cells from the two SC layers. The similarity between the two mean spectra indicates that the secondary structure of keratin, by far the major contributor to absorbance in the Amide I and II region, is essentially the same in the corneocytes isolated from the two depths. Helical secondary structure, as is predominantly found in epidermal keratin, is indicated by the frequency of the Amide I band centered at 1650 cm^{-1} in both mean spectra. It should be noted that a fraction of the intensity in this region might also be due to the Amide I and II vibrational modes from ceramide polar regions. A range of frequencies has been reported for ceramide Amide I modes (~1620–1650 cm^{-1}) depending on the particular ceramide and/or model system studied (Moore *et al.*, 1997; Rerek *et al.*, 2005). In isolated corneocytes, however, absorbance in this region owing to ceramides is expected to be relatively low compared to keratin Amide I absorbance.

Masked IR images from 72 corneocytes, 36 from each layer, were concatenated to produce the images shown in Figure 3. Within each image, the top two rows are from the corneocytes isolated from the 3rd tape strip and the bottom two rows from the 11th tape strip. The images are correlation coefficient maps calculated over the 1180–1430 cm^{-1} region between each mean spectrum (shown in Figure 2a) and the spectrum from each pixel in the original full data set. The correlation coefficients range from ~0.7 (dark blue) to 1.0 (dark red). Correlation to the mean generated from the 3rd layer (Figure 3a) and similarly for the mean from the 11th layer (Figure 3b) clearly differentiates the layer from which the majority of the corneocytes were isolated. Some inhomogeneity between the cells isolated from each layer is evident in the images. In particular, two outliers are apparent in the spectra of the corneocytes isolated from the 3rd tape strip (Figure 3b, top two rows, left side of image). The variability is thought to reflect the range of composition and structure found in native corneocytes and also to result from the accrual of artifacts from sequential tape stripping. Finally, a relatively small degree of variability is observed within many of the individual corneocytes (each consisting of a 4 × 4 pixel area within the images).

To investigate the potential effects of hexane washing on corneocytes, a different protocol was used to isolate and examine five corneocytes from two SC depths. Using the procedure referred to as the direct method (see Materials and Methods), IR images were acquired of the same corneocyte before and after hexane dousing. Representative mean spectra from single corneocytes (4 × 4 pixel area) obtained after tape stripping two (superficial) and 10 (deeper) times are displayed in Figure 4 before and after washing with hexane. Evidently, hexane washing does not produce significant changes in the spectral region (1180–1430 cm^{-1}) shown in Figure 4a. Some differences are observed, however, in spectral regions where lipids have strong absorption bands (e.g., Figure 4b, 2830–2990 cm^{-1}). For each corneocyte, Amide I band intensity was essentially unchanged (<1%) by the hexane treatment (not shown); however, some variation

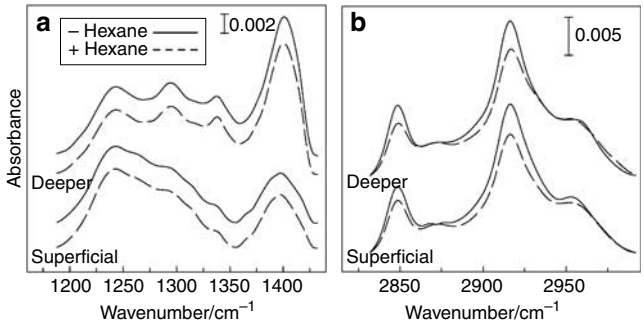

Figure 4. Mean IR spectra of corneocytes from two depths in human SC isolated using the direct method before and after washing with hexane. Mean IR spectra from a 4 × 4 pixel area of the same corneocyte obtained after tape stripping two (superficial) and 10 (deeper) times before and after hexane treatment. (**a**) 1180–1430 cm^{-1} spectral region and (**b**) 2830–2990 cm^{-1} spectral region.

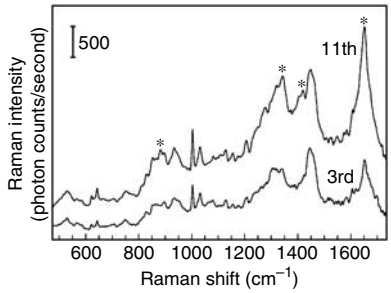

Figure 5. Mean Raman spectra of human corneocytes from two SC layers. Mean Raman spectra (475–1740 cm^{-1} region) of corneocytes isolated from 3rd (bottom spectrum) and 11th (top spectrum) tape strips obtained from human forearm skin. The asterisks mark bands or regions assigned to NMF where relative intensity significantly increases with SC depth.

between corneocytes within each layer was observed (~10%). In addition, Amide I and II band positions and shapes did not change, indicating that the secondary structure of keratin is unaltered by hexane. The band area ratio of the 1404 cm^{-1} carboxylate mode to the Amide I vibration was calculated and averaged for the five cells isolated from each layer providing a semiquantitative analysis of relative NMF concentration. After hexane treatment, the relative NMF concentration decreased by ~1.5% for corneocytes from the superficial layer and ~3.0% for the deeper layer. When compared to the differences in the relative NMF concentration between the two layers (>100%) for cells isolated using both methods, the decrease owing to hexane is insignificant. Upon examination of the CH stretching region (Figure 4b), a lipid loss of 25–30% is detected in the spectra of corneocytes from both layers as determined from the band area ratio of the symmetric methylene stretching mode (~2848 cm^{-1}) to the Amide I. It is clear from the figure that the asymmetric methylene stretching mode (~2920 cm^{-1}) behaves similarly. Evidently, this hexane-induced partial loss of noncovalently bound lipid does not promote significant leaching of the NMF components. In addition, the frequencies of both methylene stretching modes indicative of acyl chain conformational order do not change significantly (<0.5 cm^{-1}) after hexane washing. Overall, hexane was found to affect the corneocytes from both layers in a similar manner.

Further confirmation of the depth-dependent NMF loss was provided by Raman microspectroscopic measurements of several corneocytes isolated from the 3rd and 11th tape strips. Mean Raman spectra for ~8 corneocytes isolated from each of two SC layers (3rd and 11th tape strips) are presented in Figure 5. In the figure, the asterisks mark four spectral regions (882, 1342, 1400–1420, and 1650 cm^{-1}) where increased band intensities are observed for corneocytes isolated from deeper SC layers. Previous reports from the Puppels' lab based on Raman measurements of predominant NMF components have assigned the feature at ~1415 cm^{-1} to the amino acids, serine, glycine, and alanine, and the feature at ~885 cm^{-1} to pyrrolidone-5-carboxylic acid (Caspers *et al.*, 1998, 2002), a metabolic product derived from the glutamate and/or glutamine residues found in filaggrin. The band at ~1650 cm^{-1} arises from various skin constituents and at least two overlapped vibrational modes. Contributions to the Amide I mode are made by proteins, ceramides, and specific NMF constituents such as, pyrrolidone carboxylic acid, which contains an amide group. The C=C stretching mode also produces a band in this region, relatively sharper and stronger than the Amide I band. A major NMF component, urocanic acid, derived from the amino acid histidine, contains a C–C double bond conjugated with the histidine imidazole ring. The amino-acid composition of filaggrin includes approximately 5% histidine residues (Scott *et al.*, 1982). The significant difference observed in the Raman intensity of the ~1650 cm^{-1} band may in part be due to depth-dependent changes in protein, ceramide, and pyrrolidone carboxylic acid concentrations; however, a larger portion of the variation is suggested to arise from a decrease in the amount of urocanic acid present in the most superficial SC layers. The relatively smaller depth-dependent change observed in the IR Amide I band intensity (Figure 2b) supports this interpretation given that the C=C stretching vibration is very weak in the IR.

In related reports from the Puppels group, *in vivo* confocal Raman measurements provided relative concentration depth profiles for total NMF and several of its individual components in human skin from two different body sites both with relatively thick SC (~70–100 μm) (Caspers *et al.*, 2001, 2003). Concurrent with the *in vivo* measurements, the increase in the intensity of the bands with depth observed in the current Raman and IR experiments almost certainly reflects an increase in corneocyte NMF concentration in going from superficial SC regions (3rd tape strip) to the ~11th layer of cells.

An NMF concentration profile was constructed from IR images of individual corneocytes isolated from the 3rd, 6th, and 11th tape strips using the ratio of integrated band areas, 1404 cm^{-1}/Amide I. IR images of the band area ratio for the three corneocytes are shown in Figure 6a. A plot of this spectral parameter acquired along the white line drawn in Figure 6a along with the mean value for each corneocyte are displayed in Figure 6b. The data from the three corneocytes

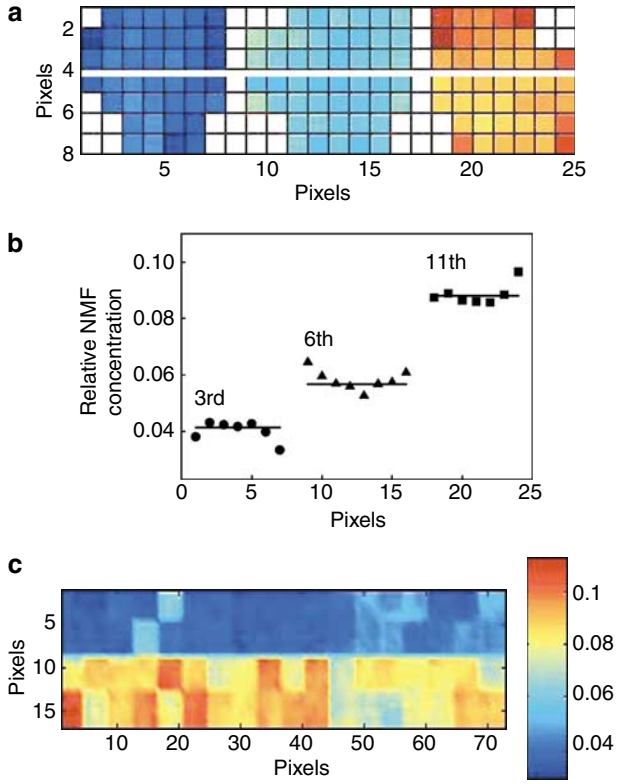

Figure 6. Relative NMF concentration profile determined from IR imaging of corneocytes isolated from different depths in human SC. (**a**) Relative NMF concentration image determined from the ratio of integrated band areas (1404 cm^{-1}/Amide I) in three corneocytes isolated from the 3rd, 6th, and 11th tape strips. The color red corresponds to higher concentration and blue to lower. (**b**) Relative NMF concentration as determined by the integrated band area ratio (1404 cm^{-1}/Amide I) along the white line drawn in (**a**). The individual data points represent the measured ratio obtained from each pixel in the image and the solid lines are the mean values for each corneocyte. (**c**) Image of relative NMF concentration for the full corneocyte data set as described in the caption for Figure 3.

show that the relative concentration of NMF more than doubles with depth in the outermost approximately 11 layers of the SC (from 0.41 to 0.88). These results are in general agreement with the outer layers sampled in the confocal Raman study mentioned above (Caspers *et al.*, 2003) and in excellent agreement with an earlier review depicting the concentration of one of the major components of NMF, pyrollidone carboxylic acid, in the outer 8 μm of the SC (Rawlings *et al.*, 1994). An image of the same band area ratio, calculated for the full corneocyte data set used herein, is presented in Figure 6c with the range of values shown in the color bar. The mean ratio for the 3rd layer is 0.041 with a standard deviation of 0.007 and 0.086 ± 0.010 for the 11th layer. The IR spectral parameter provides a measure of relative NMF concentration that is observed to differ significantly with SC depth.

DISCUSSION

Significant efforts are underway to develop vibrational spectroscopic imaging applications that are useful to the biomedical community. Several approaches are being taken to investigate the competency of the techniques for detecting the initial stages of disease, understanding molecular changes accompanying disease, and defining the effects of therapeutic intervention on a molecular level. Towards this end, the ability to delineate biochemical composition and molecular events within a single cell should prove very useful. Acquiring molecular level information using *in vivo* sampling is another valuable approach.

The current work demonstrates the feasibility of acquiring molecular level biochemical and structural information from single corneocytes sampled at different points in the maturation and exfoliation process. In healthy skin, the complex process of complete cell turnover takes $\sim$30 days. Most notably, the present work reveals the depth dependence of NMF concentration in the outer $\sim 6\,\mu$m of the SC.

NMF components are thought to facilitate critical biochemical events in the SC. Perturbations in NMF concentration have been linked to aging, surfactant exposure, and disease states of varying severity. Thus, the quantification of the NMF concentration gradient in the SC will provide meaningful information to the medical, pharmaceutical, and cosmetic industries. *In vivo* confocal Raman measurements of human skin have been reported delineating NMF and water concentration profiles at body sites known to have a thick SC (Caspers *et al.*, 2002, 2003). This noninvasive approach coupled with confocal laser scanning microscopy has shown that both profiles are directly related to skin architecture (Caspers *et al.*, 2003). The results are consistent with an earlier report finding that a decrease in water concentration is required before filaggrin proteolysis to form NMF (Scott and Harding, 1986) as occurs at the junction of the SC and viable epidermis. The *in vivo* Raman measurements were conducted using depth increments of 10 μm up to a total depth of $\sim 150\,\mu$m from the skin surface. The methodology used in the current work essentially increases the axial resolution (in the superficial SC region sampled), as one tape strip removes approximately one layer of corneocytes ($\sim 0.5\,\mu$m). In general, the consistency between the results of the different sampling protocols and spectroscopic methods provides a high level of confidence in the sampling and measurement protocols used in both laboratories.

Skin pathologies such as psoriasis, atopic dermatitis, and ichthyosis vulgaris display abnormal desquamation processes where the amount of NMF is greatly decreased or is absent (Rawlings *et al.*, 1994). In a report comparing SC biopsies from the heels of healthy subjects and from the symptom-free heels of patients with active psoriasis, Raman spectra show a significant decrease in the relative intensity of a band at $\sim 1418\,cm^{-1}$ (Wohlrab *et al.*, 2001), which may be interpreted as a decrease in NMF. A more recent Raman study comparing healthy and psoriatic skin reported disruption in lipid conformational order and suggested unfolding of proteins in psoriatic samples (Osada *et al.*, 2004). In psoriasis, it is not entirely clear whether a malfunctioning barrier is the driving force or the consequence of keratinocyte hyperproliferation and immune-mediated inflammatory responses (Ghadially *et al.*, 1996; Lebwohl, 2003). In either case,

spectral parameters such as that derived to measure relative NMF concentrations, along with established markers of protein secondary structure and lipid order could be used to evaluate therapeutic interventions.

Vibrational imaging techniques may not only prove useful in evaluating disease states, but as demonstrated here, may also clarify results obtained using common procedures. Organic solvents and other agents are often used as permeation enhancers or in experimental protocols to evaluate barrier function. The effects of particular agents on extracting SC lipids have been reported (Abrams *et al.*, 1993), but it is generally more difficult to access molecular structure alterations. In the current work, use of the solvent hexane is shown to preserve corneocyte NMF concentration and keratin secondary structure while partial removal of non-covalently bound lipid occurs (Figure 4). Although the hexane-induced extraction of some SC lipids was anticipated from previous reports on skin biopsies (Abrams *et al.*, 1993), the maintenance of keratin structure and NMF concentration was unknown.

These initial studies identify several IR and Raman spectral parameters to evaluate relative NMF and lipid concentrations together with lipid and protein conformation in individual corneocytes. Additional sampling with variations in gender and age of subjects, for instance, will aid in assessing the statistical robustness of the parameters. Further investigations may also provide a clearer picture of the corneocyte maturation process from which various therapeutic interventions in the treatment of skin disorders can be evaluated.

MATERIALS AND METHODS

Preparation of corneocytes

The Rutgers University Internal Review Board has approved all protocols used herein. The ethical principles for nonclinical biomedical research involving human subjects as declared in the Declaration of Helsinki Principles were adhered to and consent from the subject was obtained. Corneocytes from different layers of the SC were collected from the same site of human forearm skin by sequential tape stripping (Sellotape, 3 M Scotchguard) an area of approximately 2.5×15 cm. The forearm area was flushed with water for several minutes before tape stripping. The first two tape strips were discarded and corneocytes collected from the 3rd, 6th, and 11th tape strips were prepared as follows. Corneocytes were flushed off the tape into a beaker using HPLC grade hexane. The corneocyte/hexane suspension was sonicated for 5 minutes to break up the desmosomal and lipid cohesion between individual corneocytes. The corneocytes were then isolated using nitrocellulose membrane filters (GE Osmonics Labstore, Minnetonka, MN; pore size 0.22 μm). Corneocytes were rinsed and resuspended using fresh hexane. This procedure was repeated three times to ensure that all glue had been removed. Corneocytes were harvested and isolated on several separate occasions. Aliquots of this corneocyte suspension, containing some noncovalently bound lipids, were deposited on either CaF_2 windows for IR imaging or gold-coated silicon substrates for Raman measurements. The majority of the results presented herein used this method for corneocyte isolation. All samples were dried overnight under house vacuum before measurements were made.

A smaller number of corneocytes were isolated using a more difficult protocol, referred to as the direct method, to specifically evaluate the effect of hexane on individual corneocyte composition and the molecular structure of cell constituents. This method is inconvenient for scaling up to evaluate the numbers of corneocytes necessary for statistical data analysis, but it does serve as an appropriate protocol for the analysis of control samples. Corneocytes were directly collected from human forearm skin by pressing a CaF_2 window on the site after tape stripping and gently rubbing the skin with a cotton tip. A few free corneocytes stuck to the window after tape stripping the site two and 10 times. Corneocytes are designated as being isolated from either a superficial or deeper SC layer (see Results), as it seems as if the assignment of corneocytes to a specific SC layer is less certain compared to the first tape stripping protocol described above. Using the light microscope portion of the Perkin-Elmer Spotlight instrument, single corneocytes were marked and IR images were acquired of the same corneocyte before and after continuously soaking the cell with small aliquots of hexane (total volume 50 μl) for approximately 10 minutes. A final 10 μl hexane flush was applied to each corneocyte before drying the sample and IR data collection. Residual hexane was not detected in the spectra.

Preparation of NMF film

Chemicals were purchased from Sigma-Aldrich (St Louis, MO) and the dry powders were combined as follows (in weight %): serine (30%), glycine (18%), pyrrolidone carboxylic acid (16%), alanine (11%), histidine (7%), ornithine (6%), citruline (5%), arginine (5%), and proline (2%). These relative concentrations roughly reflect the amino-acid composition of filaggrin (Rawlings *et al.*, 1994) and are in general agreement with previously published *in vivo* studies of human NMF composition (Caspers *et al.*, 2001). A solution was prepared in distilled water at pH 5.5, spread on to a CaF_2 window, and allowed to dry overnight at room temperature to a gel-like film.

IR imaging

IR microscopic images were acquired with the Perkin-Elmer Spotlight system, which consists of an essentially linear array (16×1 detector elements) mercury–cadmium–telluride detector along with an automated high-precision XY sample stage. About 50 corneocytes from each layer were randomly selected and IR images ($\sim 60 \times 60\ \mu m^2$) were acquired with a pixel size of 6.25 μm and spatial resolution of 10–12 μm. Thirty-two scans were collected for each spectrum using 8 cm^{-1} spectral resolution and one level of zero-filling yielding data encoded at 4 cm^{-1} intervals. Each corneocyte image was acquired in $\sim$20 minutes.

Raman microscopy

Raman spectra of corneocytes were acquired with a Kaiser Optical Systems Raman Microprobe. The instrument has confocal sampling capability and has been previously described in detail (Xiao *et al.*, 2004). A solid-state diode laser (785 nm excitation wavelength) generates $\sim$4–7 mW of single mode power at the sample. The back-scattered light is collected from a spot size of $\sim 2\ \mu$m and illuminates a thermoelectrically cooled, near-IR CCD (ANDOR Technology, Model DU 401-BR-DD). Spectral coverage is from 100 to 3450 cm^{-1} at spectral resolution of 4 cm^{-1} and data are encoded every 0.3 cm^{-1}. Acquisition time for each spectrum was $\sim$10 minutes (including

cosmic-ray correction) and 10–15 corneocytes from each layer were sampled.

Data analysis

Grams/32 AI software version 6.0 (Thermo Galactic, Salem, NH) was used for processing Raman spectra. Raman spectra from each layer were averaged, Fourier smoothed (80%), and linear baselines were applied. Processed mean spectra were compared to the raw data to ensure that spectral features were not misrepresented. As the original data are encoded every 0.3 cm^{-1}, the relatively large degree of Fourier smoothing could be applied without distorting the spectra.

Spectral Dimensions (Olney, MD) ISys 3.0 software was used for the analysis and construction of the IR images. Linear baselines were applied over spectral regions of interest. Data interpretation was facilitated by averaging the spectra of corneocytes from particular SC layers to improve signal-to-noise ratios. Correlation coefficients were then calculated between the mean spectrum of each layer and each spectrum contained in an image to generate correlation maps.

CONFLICT OF INTEREST

The authors state no conflict of interest.

ACKNOWLEDGMENTS

This work was supported by PHS Grant GM 29864 to RM.

REFERENCES

Abrams K, Harvell JD, Shriner D, Wertz P, Maibach H, Maibach HI *et al.* (1993) Effect of organic solvent on *in vitro* human skin water barrier function. *J Invest Dermatol* 101:609–13

Caspers PJ, Lucassen GW, Carter EA, Bruining HA, Puppels GJ (2001) *In vivo* confocal Raman microspectroscopy of the skin: Noninvasive determination of molecular concentration profiles. *J Invest Dermatol* 116: 434–41

Caspers PJ, Lucassen GW, Puppels GJ (2003) Combined *in vivo* confocal Raman spectroscopy and confocal microscopy of human skin. *Biophys J* 85:572–80

Caspers PJ, Lucassen GW, Wolthuis R, Bruining HA, Puppels GJ (1998) *In vitro* and *in vivo* Raman spectroscopy of human skin. *Biospectroscopy* 4:S31–9

Caspers PJ, Williams AC, Carter EA, Edwards HG, Barry BW, Bruining HA *et al.* (2002) Monitoring the penetration enhancer dimethyl sulfoxide in human stratum corneum *in vivo* by confocal Raman spectroscopy. *Pharm Res* 19:1577–80

Elias PM (1991) Epidermal barrier function: intercellular lamellar lipid structures, origin, composition and metabolism. *J Contr Rel* 15:199–208

Gerger A, Koller S, Kern T, Massone C, Steiger K, Richtig E *et al.* (2005) Diagnostic applicability of *in vivo* confocal laser scanning microscopy in melanocytic skin tumors. *J Invest Dermatol* 124:493–8

Ghadially R, Reed JT, Elias PM (1996) Stratum corneum structure and function correlates with phenotype in psoriasis. *J Invest Dermatol* 107:558–64

Hanson KM, Behne MJ, Barry NP, Mauro TM, Gratton E, Clegg RM (2002) Two-photon fluorescence lifetime imaging of the skin stratum corneum pH gradient. *Biophys J* 83:1682–90

Krimm S, Bandekar J (1986) Vibrational spectroscopy and conformation of peptides, polypeptides, and proteins. *Adv Protein Chem* 38:181–363

Langley RGB, Rajadhyaksha M, Dwyer PJ, Sober AJ, Flotte TJ, Anderson RR (2001) Confocal scanning laser microscopy of benign and malignant melanocytic skin lesions *in vivo*. *J Am Acad Dermatol* 45:365–76

Lebwohl M (2003) Psoriasis. *Lancet* 361:1197–204

Moore DJ, Rerek ME, Mendelsohn R (1997) FTIR spectroscopy studies of the conformational order and phase behavior of ceramides. *J Phys Chem B* 101:8933–40

Moss DA, Keese M, Pepperkok R (2005) IR microspectroscopy of live cells. *Vib Spectrosc* 38:185–91

Osada M, Gniadecka M, Wulf HC (2004) Near-infrared Fourier transform Raman spectroscopic analysis of proteins, water and lipids in intact normal stratum corneum and psoriasis scales. *Exp Dermatol* 13:391–5

Rawlings AV, Scott IR, Harding CR, Bowser PA (1994) Stratum corneum moisturization at the molecular level. *J Invest Dermatol* 103:731–40

Rerek ME, Van Wyck D, Mendelsohn R, Moore DJ (2005) FTIR spectroscopic studies of lipid dynamics in phytosphingosine ceramide models of the stratum corneum lipid matrix. *Chem Phys Lipids* 134:51–8

Salzer R, Steiner G, Mantsch HH, Mansfield J, Lewis EN (2000) Infrared and Raman imaging of biological and biomimetic samples. *Fresen J Anal Chem* 366:712–6

Schaefer H, Redelmeier TE (1996) *Skin barrier: principles of percutaneous absorption*. Basel: Karger

Scott IR, Harding CR (1986) Filaggrin breakdown to water binding compounds during development of the rat stratum corneum is controlled by the water activity of the environment. *Dev Biol* 115:84–92

Scott IR, Harding CR, Barrett JG (1982) Histidine-rich proteins of the keratohylain granules. Source of the free amino acids, urocanic acid and pyrrolidone carboxylic acid in the stratum corneum. *Biochim Biophys Acta* 719:110–7

So PTC, Dong CY, Masters BR, Berland KM (2000) Two-photon excitation fluorescence microscopy. *Annu Rev Biomed Eng* 2:399–429

Wohlrab J, Vollmann A, Wartewig S, Marsch WC, Neubert R (2001) Noninvasive characterization of human stratum corneum of undiseased skin of patients with atopic dermatitis and psoriasis as studied by Fourier transform Raman spectroscopy. *Biopolymers* 62:141–6

Xiao C, Flach CR, Marcott M, Mendelsohn R (2004) Uncertainties in depth determination and comparison of multivariate with univariate analysis in confocal Raman studies of a laminated polymer and skin. *Appl Spectrosc* 58:382–9

Xiao C, Moore DJ, Rerek ME, Flach CR, Mendelsohn R (2005) Feasibility of tracking phospholipid permeation into skin using infrared and Raman microscopic imaging. *J Invest Dermatol* 124:622–32

Yu B, Kim KH, So PTC, Blankschtein D, Langer R (2003) Visualization of oleic acid-induced transdermal diffusion pathways using two-photon fluorescence microscopy. *J Invest Dermatol* 120:448–55